

## Fabrication and Characterization of Nano-TCP Doped with Various Ions for Bone Implant Applications

Serap GÜNGÖR KOÇ<sup>1\*</sup> Redar Wasurahman AHMED<sup>1</sup>

**ABSTRACT:** Calcium phosphate (CaP) based bioceramics are frequently used in dental and orthopedic field as bone grafts due to their chemical and structural similarities to the human hard tissues. Strontium ( $Sr^{2+}$ ), fluoride ( $F^-$ ) and chloride ( $Cl^-$ ) ions are known to play important role in bone and tooth microstructure. The aim of this study was to combine tri-calcium phosphates doped with strontium, chloride and fluoride ions. A precipitation procedure was applied for synthesizing pure and doped tri-calcium phosphates. The undoped and doped samples were sintered at 1100°C for 1 h. Incorporation of the strontium ( $Sr^{+2}$ ) and chloride ( $Cl^-$ ) ions decreased the density of the samples while, the fluoride ( $F^-$ ) co-doped densities increased with respect to pure TCP. The XRD results revealed the existence of the  $\alpha$ -TCP and  $\beta$ -TCP phases. SEM results confirmed the sintering temperature and amount of dopants had prominent effect on the grain sizes of the samples.

**Keywords:** Biomaterials, chloride, fluoride, precipitation method, strontium, tri-calcium phosphate.

### Kemik İmplant Uygulamalarında Kullanılmak Üzere Çeşitli İyonlar Eklenmiş Nano-Trikalsiyum Fosfatların Üretimi ve Karakterizasyonu

**ÖZET:** Diş ve ortopedik protezlerin üretiminde kalsiyum fosfat (CaP) bazlı biyoseramikler sıklıkla kullanılmaktadır. Özellikle, kemiğin kimyasal ve yapısal benzerliklerinden dolayı tercih edilmektedirler. Stronsiyum ( $Sr^{2+}$ ), florür ( $F^-$ ) ve klorür ( $Cl^-$ ) iyonlarının kemik ve dişlerin metabolizmasında ve yapısında önemli rol oynadığı bilinmektedir. Bu çalışmanın amacı stronsiyum, klorür ve florür iyonları ile katkılandırılmış tri-kalsiyum fosfatların üretilmesidir. Saf ve katkılandırılmış tri-kalsiyum fosfatlar çöktürme yöntemi kullanılarak sentezlenmiştir. Katkısız ve katkılandırılmış numuneler 1 saat süresince 1100°C 'de sinterlenmiştir. Stronsiyum ( $Sr^{+2}$ ) ve klorürün ( $Cl^-$ ) ilavesi ile numunelerin yoğunluğunu azalırken, florür ( $F^-$ ) miktarının artmasıyla numunelerin yoğunluklarında artış gözlemlenmiştir. XRD sonuçları  $\alpha$ -TCP ve  $\beta$ -TCP fazlarının varlığını ortaya koymuştur. SEM görüntüleri sinterleme sıcaklığının ve katkılandırılan iyon miktarlarının numuneler üzerindeki tane büyüklüklerine anlamlı bir etkiye sahip olduğunu doğrulamaktadır.

**Anahtar kelimeler:** Biyomalzemeler, klor, flor, çöktürme yöntemi, stronsiyum, tri-kalsiyum fosfat.

<sup>1</sup> Serap GÜNGÖR KOÇ (Orcid ID: 0000-0002-4547-0642), Redar Wasurahman AHMED (Orcid ID: 0000-0001-7375-4178), Van Yuzuncu Yıl University, Faculty of Engineering, Department of Mechanical Engineering, Van, Turkey

\*Sorumlu Yazar / Corresponding Author: Serap GÜNGÖR KOÇ, e-mail: serapgungor@yyu.edu.tr

This study is a part of the Master thesis of Redar Wasurahman AHMED

## INTRODUCTION

Chemical similarity of  $\beta$ -TCP ( $\beta$ -tricalcium phosphate) to the mineral component of bone is the key reason behind the usage of  $\beta$ -TCP as replacement materials (LeGeros et al., 2002; 2003). Thus, in several surgical fields like orthopedic and dental surgeries,  $\beta$ -TCP has been used as bone filling material (Park and Lakes, 1992). This resulted in a physicochemical bond in between the bone and osteo-integration implants (Metseger et al., 1999). Nonetheless,  $\beta$ -TCP mechanical properties are the main restriction to the utilization of  $\beta$ -TCP as load bearing biomaterial. Furthermore, the mechanical properties of tri-calcium phosphate are commonly insufficient. When it used for making highly porous ceramics and scaffolds, its poor mechanical behavior is even high. Especially for enhancing mechanical properties of  $\beta$ -TCP, metal oxides ceramics, strontium oxide SrO as well as several oxides  $ZrO_2$ ,  $SiO_2$  have been extensively examined because of their bioinertness, excellent tribological properties, high wear resistance, fracture toughness and strength and comparatively low friction. Nonetheless, for enhancing the densification and the mechanical properties of  $\beta$ -TCP, bioinert ceramic oxides have been used. The TCP has three polymorphs, like:  $\beta$ -TCP is constant under  $1180^\circ\text{C}$ ,  $\alpha$ -TCP between  $1180^\circ\text{C}$  and  $1400^\circ\text{C}$  and  $\bar{\alpha}$ -TCP more than  $1470^\circ\text{C}$ . Amongst the three allotropic configurations,  $\beta$ -TCP is preferred as a bioceramic because of its chemical constancy, mechanical strength, and appropriate bio-resumption properties (Kannan et al., 2008).  $\beta$ -TCP crystallize in the rhombohedral crystal system and mostly utilized as a part of mono- or biphasic bioceramics and composites (Carrodeguas et al., 2011, Taktak R et al., 2018).

Strontium ions ( $\text{Sr}^{2+}$ ) replaced with the  $\text{Ca}^{2+}$  ion in the  $\beta$ -TCP microstructure. It is one of the trace element in the human skeleton (Verberckmoes et al., 2004). Strontium used mostly in the osteoporotic patients in order to

raise vertebral bone density (Bose et al., 2013). Trace amount of strontium can increase bone formation, while high amounts stimulate defective bone mineralization (Grynpas et al., 1996)

Fluoride ( $\text{F}^-$ ) is frequently used in patients with osteoporosis and dental applications in order to increase cell proliferation (Nakade et al., 1999). Co-doping of HA with fluoride ( $\text{F}^-$ ) ions resulted in serious alterations in solubility and density parameters (Cheng et al., 2005). Increased amount of the fluoride ( $\text{F}^-$ ) in HA structure will affect the mechanical properties negatively (Gross et al., 2004).

In the literature,  $\text{Cl}^-$  co-doped hydroxyapatite samples were mostly produced using combustion method, which demonstrated that the a-axis parameter of the  $\text{Cl}^-$  doped samples increased gradually with the increase in  $\text{Cl}^-$  concentration. Pure chlorapatite ions rising the acidity of the environment therefore chloride doped hydroxyapatite preferred for biomedical applications (Zhao et al., 2014). When chlorine inserted into the lattice parameters, a-axis parameter of the  $\text{Cl}^-$  doped samples increased gradually with the increase in  $\text{Cl}^-$  concentration (Kannan et al., 2006).

The ions with ( $\text{Ca}^{2+}$ ,  $\text{Ba}^{2+}$ ,  $\text{Sr}^{2+}$ ,  $\text{Mn}^{2+}$ ,  $\text{F}^-$ ,  $\text{Cl}^-$ ,  $\text{OH}^-$ ) diagnostic, antibacterial, biocompatible, mechanically strengthening and phase stabilizing specifications can be doped into the TCP to develop new implants and coating elements. There are only few studies in the literature about co-doping CaP's with more than two ions. The reason is that, when ions are doped together, their multiple-effect would not be a simple because the dopant ions changed the microstructure of doped CaP's. The purpose of this study is to synthesize TCP doped with strontium ( $\text{Sr}^{2+}$ ), chloride ( $\text{Cl}^-$ ) and fluoride ( $\text{F}^-$ ) ions for developing novel nanocomposite bioceramics for microstructure of TCP to develop biomedical applications and investigation of their microstructures and mechanical properties.

## MATERIALS AND METHODS

Pure and doped  $\beta$ -TCP powders were synthesized by a precipitation method. Reagent-grades of calcium nitratetetrahydrate ( $\text{Ca}(\text{NO}_3)_2 \cdot 4\text{H}_2\text{O}$ ) and di-ammonium hydrogen phosphate ( $(\text{NH}_4)_2\text{HPO}_4$ ) were added into distilled water to prepare the mixing solutions with a certain molar ratio. These two precursor powders were dissolved separately in distilled water with different amounts to obtain a theoretical Ca/P ratio which is 1.50. Ammonia was added into  $(\text{NH}_4)_2\text{HPO}_4$  solution after previous solutions were stirred for 1h where ammonia solution was added into both solutions to bring the pH level to 11-12. Ammonia,  $\text{Ca}(\text{NO}_3)_2 \cdot 4\text{H}_2\text{O}$  solutions, ammonium fluoride ( $\text{NH}_4\text{F}$ ), calcium chloride ( $\text{CaCl}_2$ ) and strontium nitrate ( $\text{Sr}(\text{NO}_3)_2$ ) were added at the same time

into the  $(\text{NH}_4)_2\text{HPO}_4$ -ammonia mixture in a drop wise manner after stirring for 10 minutes. The pH of the solutions was kept in the pH range 10-11 by adding ammonia solution. The resulting mixture was heated until boiling. After boiling, the mixture was left for stirring for 24h. After 1 day of aging, solution was filtered to obtain a wet cake. The wet cake was dried in an oven at 200 °C to remove the excess water and ammonia. In addition to precursors of  $\text{Ca}(\text{NO}_3)_2 \cdot 4\text{H}_2\text{O}$ ,  $(\text{NH}_4)_2\text{HPO}_4$  and  $\text{NH}_4\text{F}$ ,  $\text{CaCl}_2$  and  $\text{Sr}(\text{NO}_3)_2$  used as resources of  $\text{F}^-$ ,  $\text{Cl}^-$  and  $\text{Sr}^{+2}$ , respectively. The precipitated, dried CaPs bulks were crushed with an agate mortar and pestle. The resulting powders formed in pellets were sintered at 1100°C in air for 1h. Descriptions of pure and doped CaPs according to their strontium, chloride and fluoride compositions synthesized are given in *Table 1*.

**Table 1:** Experimental groups and mole percentages of dopants in the samples.

Sample Names	Ca/P ratio	Sr % mole	Cl % mole	F % mole
1.5TCP	1.5	0.0	0.0	0.0
1.5TCP 1.0Sr 1.0Cl 1.0F	1.5	1.0	1.0	1.0
1.5TCP 2.5Sr 1.0Cl 1.0F	1.5	2.5	1.0	1.0
1.5TCP 5.0Sr 1.0Cl 1.0F	1.5	5.0	1.0	1.0
1.5TCP 10.0Sr 1.0Cl 1.0F	1.5	10.0	1.0	1.0
1.5TCP 2.5Sr 2.5Cl 1.0F	1.5	2.5	2.5	1.0
1.5TCP 2.5Sr 5.0Cl 1.0F	1.5	2.5	5.0	1.0
1.5TCP 2.5Sr 10.0Cl 1.0F	1.5	2.5	10.0	1.0
1.5TCP 2.5Sr 2.5Cl 1.0F	1.5	2.5	2.5	1.0
1.5TCP 2.5Sr 2.5Cl 2.5F	1.5	2.5	2.5	2.5
1.5TCP 2.5Sr 2.5Cl 5.0F	1.5	2.5	2.5	5.0

Densities of the sintered samples were derived by Archimedes method. Dry weight and the weight in distilled water were measured. The density of the samples was calculated according to the below formula:

$$\text{Density (g cm}^{-3}\text{)} = \frac{W_{t(\text{air})}}{W_{t(\text{air})} - W_{t(\text{water})}} \times \rho_{(\text{water})} \quad (1)$$

Where  $W_{t(\text{air})}$  is mass of the sample in the air and  $W_{t(\text{water})}$  is mass of the sample in the water. Phases present in the pure and doped samples were obtained by XRD. XRD (PANalytical: Empyrean) was performed on the samples with a

Cu-K $\alpha$  radiation at 40kV/40mA and samples were scanned from 10° to 80° in 2 $\theta$  with a scanning step size of 2,0°/min. JCPDS (Joint committee on powder diffraction standards) files were used for comparison with the positions of diffracted planes taken from XRD results. Presence of phases in pure and doped CaPs was calculated by using relative intensity measurements of diffracted planes. Grain size and morphology of the prepared samples were determined by SEM (Zeiss, Sigma 300) at a

voltage of 20 kV. Before to the SEM analysis, the samples were coated with gold and palladium.

## RESULTS AND DISCUSSION

XRD patterns of the synthesized powders are given in Fig. 1- Fig. 3. As seen in the XRD patterns, main phase of the samples were  $\beta$ -TCP. By adding 2.5% mole of  $\text{Sr}^{+2}$  ion, narrow peaks

appeared to be highly crystalline. It was observed that  $\text{Sr}^{+2}$  ion substitution resulted in an increase in peak intensities of  $\beta$ -TCP and  $\alpha$ -TCP (Figure 2), when the amount of the  $\text{Sr}^{+2}$  increased from 2.5 to 5.0% mole, peak intensities decreased, even in some places  $\alpha$ -TCP peaks nearly disappeared by the existence of high amount of  $\text{Sr}^{+2}$  ions.

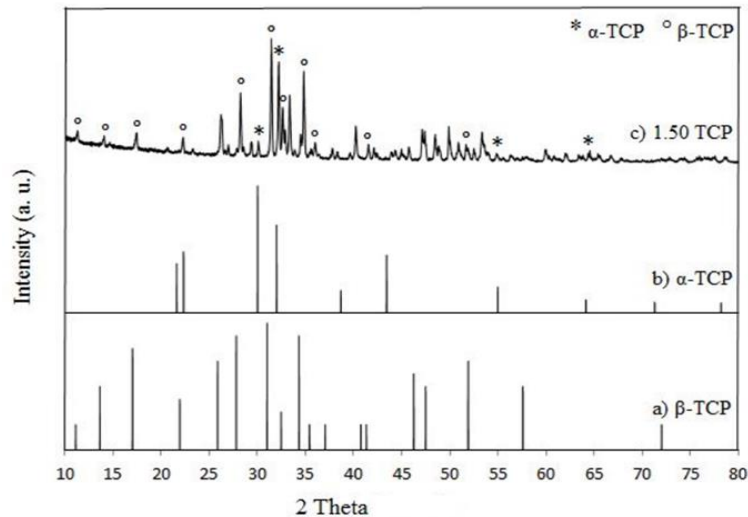


**Figure 1.** XRD patterns of 1.50 TCP (a)  $\beta$ -TCP of JCPDS # 09-0169 (b)  $\alpha$ -TCP of JCPDS # 09-0348 (c) 1.50 TCP.

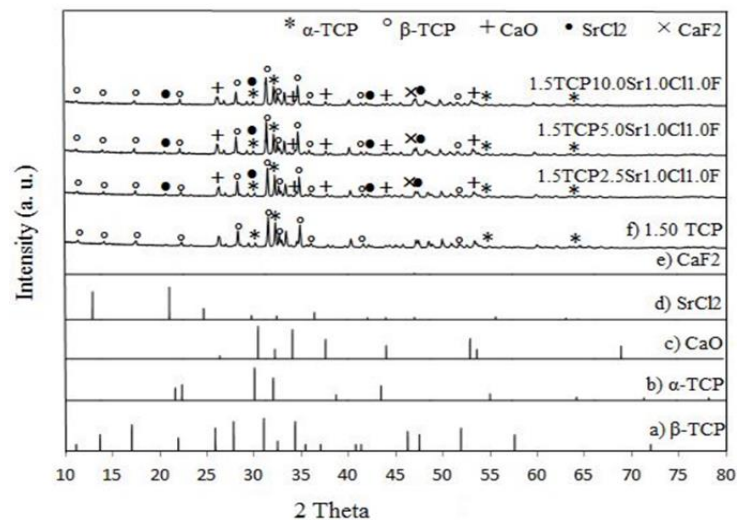


**Figure 2.** XRD patterns of doped 1.50TCP2.5Sr1.0Cl1.0F, 1.50TCP5.0Sr1.0Cl1.0F and 1.50TCP10.0Sr0Cl1.0F (a)  $\beta$ -TCP of JCPDS # 09-0169 (b)  $\alpha$ -TCP of JCPDS # 09-0348 (c) CaO of JCPDS # 01-076-8925 (d)  $\text{SrCl}_2$  of JCPDS # 01-074-0523 (e)  $\text{CaF}_2$  of JCPDS # 01-070-2739 (f) 1.50 TCP.

As seen in Figure 3, when the amount of strontium and chloride increased to 2.5% mole, the peak intensities of the  $\beta$ -TCP and  $\alpha$ -TCP decreased and that is expected to improve the mechanical properties like elastic modulus and shrinkage of materials that depending on the

crystalline of the materials (Kutbay et al., 2014). However, when the amount of the chloride increased to 2.5% mole, the intensity of the peaks increased due to the loss of strength and nonhomogeneous shape of crystalline.

The presence of  $\alpha$ -TCP and  $\beta$ -TCP phases, resulted from increasing the amount of the Cl<sup>-</sup> ions from 2.5% to 5.0% mole. When Cl<sup>-</sup> amount increased 2.5% to 5.0% mole, the existence of  $\alpha$ -TCP increased in comparison to  $\beta$ -TCP phase. This indicated that the structural stability improved by the addition of Cl<sup>-</sup> ion to calcium

phosphates. Furthermore, the presence of 1.0% F<sup>-</sup> in the Sr<sup>+2</sup> doped TCP altered the Sr<sup>+2</sup> quantity from 5.0% to 10.0% mole. As shown in Figure 4, the peak intensities of  $\beta$ -TCP increased and the peak of the  $\alpha$ -TCP in the samples decreased with the increasing amount of F<sup>-</sup> from 2.5% to 5.0% mole.

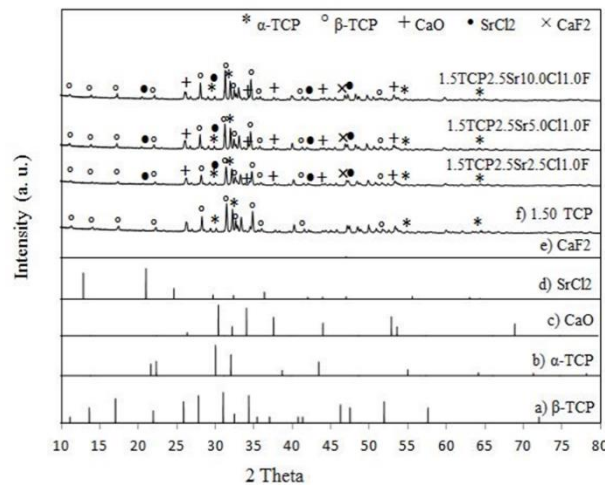


**Figure 3.** XRD patterns of doped 1.50TCP2.5Sr2.5Cl11.0F, 1.50TCP2.5Sr5.0Cl11.0F and 1.50TCP2.5Sr10.0Cl11.0F. (a)  $\beta$ -TCP of JCPDS # 09-0169 (b)  $\alpha$ -TCP of JCPDS # 09-0348 (c) CaO of JCPDS # 01-076-8925 (d) SrCl<sub>2</sub> of JCPDS # 01-074-0523 (e) CaF<sub>2</sub> of JCPDS # 01-070-2739 (f) 1.50 TCP.

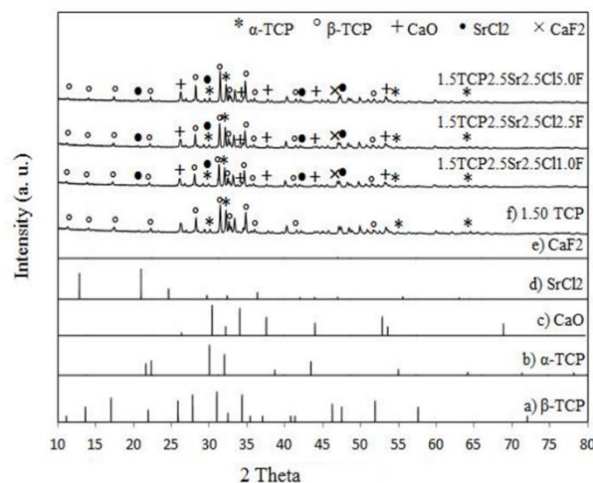


**Figure 4.** XRD patterns of doped 1.50TCP2.5Sr2.5Cl11.0F, 1.50TCP2.5Sr2.5Cl12.5F and 1.50TCP2.5Sr2.5Cl15.0F (a)  $\beta$ -TCP of JCPDS # 09-0169 (b)  $\alpha$ -TCP of JCPDS # 09-0348 (c) CaO of JCPDS # 01-076-8925 (d) SrCl<sub>2</sub> of JCPDS # 01-074-0523 (e) CaF<sub>2</sub> of JCPDS # 01-070-2739 (f) 1.50 TCP.

SEM images (200nm) shown in Figure 5, 6, 7 reveal that significant amount of porosity are obvious in both pure TCP and doped samples. This explains the minor bulk densities for those compositions. This is obvious that throughout the sintering process, substantial grain growth in TCP samples observed due to the presence of SrCl<sub>2</sub>.

This might be because of the phosphorous atoms replacing Ca<sup>+2</sup> ions. The oxygen gaps are attracted by some substitutional ions that results in elevated balance concentration of gaps.

This process generates faster grain development throughout sintering process. Fine grains and more uniform microstructures are

observed in SEM images on the samples sintered at 1100°C. It is obvious that, there is a relationship between sintering temperature and amount of the dopants. As shown in Figure 5 that grain sizes were grown up by increasing the  $\text{Sr}^{+2}$

amount from 1.0% mole to 5.0% mole, when compared to the pure TCP. Furthermore, higher sizes of grains were determined in the samples when TCP doped with  $\text{Sr}^{+2}$  compared to pure TCP.

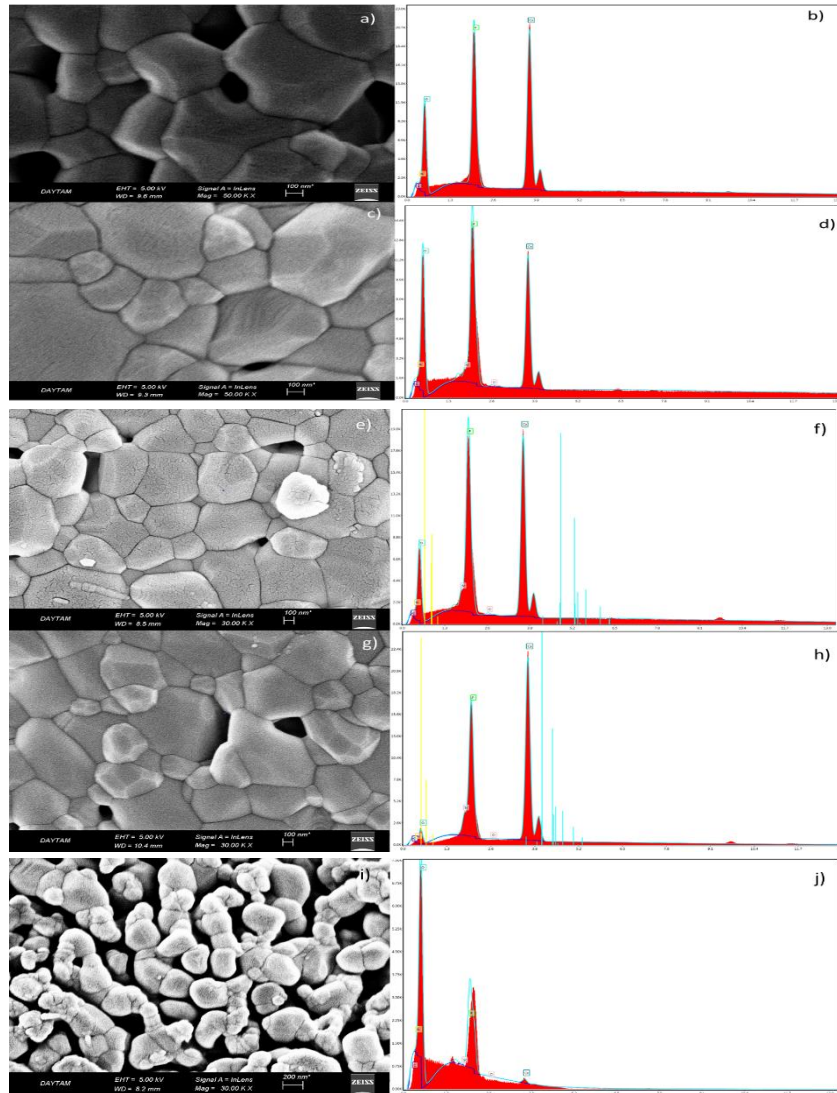


**Figure 5.** SEM and EDS images of synthesized samples (100nm). (a, b) 1.50TCP (c, d) 1.5TCP1.0Sr1.0Cl1.0F (e, f) 1.5TCP2.5Sr1.0Cl1.0F (g, h) 1.5TCP5.0Sr1.0Cl1.0F (i, j) 1.5TCP10Sr1.0Cl1.0F.

Densities of pure and doped TCP with ions ( $\text{Sr}^{+2}$ ,  $\text{Cl}^-$  and  $\text{F}^-$ ) were obtained between 2.4979  $\text{g cm}^{-3}$  to 4.0632  $\text{g cm}^{-3}$ . Although all the densities of co-doped samples were close to that of pure TCP, increasing the amount of  $\text{Sr}^{2+}$  ions caused a small decrease (1.0% mole  $\text{Sr}^{2+}$  and 5% mole  $\text{Sr}^{2+}$ ) in the density at first, but when the amount of  $\text{Sr}^{2+}$  ions was further increased, the density increased (2.5% mole  $\text{Sr}^{2+}$  and 10% mole  $\text{Sr}^{2+}$ ) with respect to pure TCP. Moreover, with increasing the amount of the chloride ( $\text{Cl}^-$ ) ions

caused a serious decrease in the density (2.4979  $\text{g cm}^{-3}$ ) as shown in Table 2. Furthermore, among other samples, 1.5TCP2.5Sr2.5Cl2.5F exhibited the highest density (4.0632  $\text{g cm}^{-3}$ ). With increasing the amount of the fluoride ( $\text{F}^-$ ) ions, some of the strontium ( $\text{Sr}^{2+}$ ) and chloride ( $\text{Cl}^-$ ) co-doped sample densities decreased with respect to pure TCP which could be due to decrease of a decomposition rate of materials that shows the highest thermal stability.

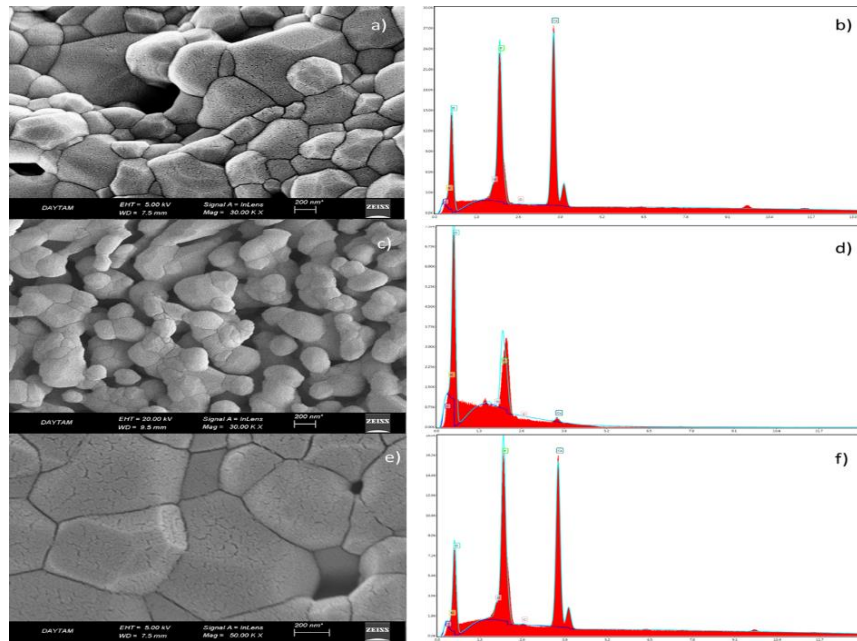


**Figure 6.** SEM and EDS images of synthesized samples (200nm). (a,b) 1.5TCP2.5Sr2.5Cl1.0F (c,d) 1.5TCP2.5Sr5.0Cl1.0F (e,f) 1.5TCP2.5Sr10Cl1.0F.

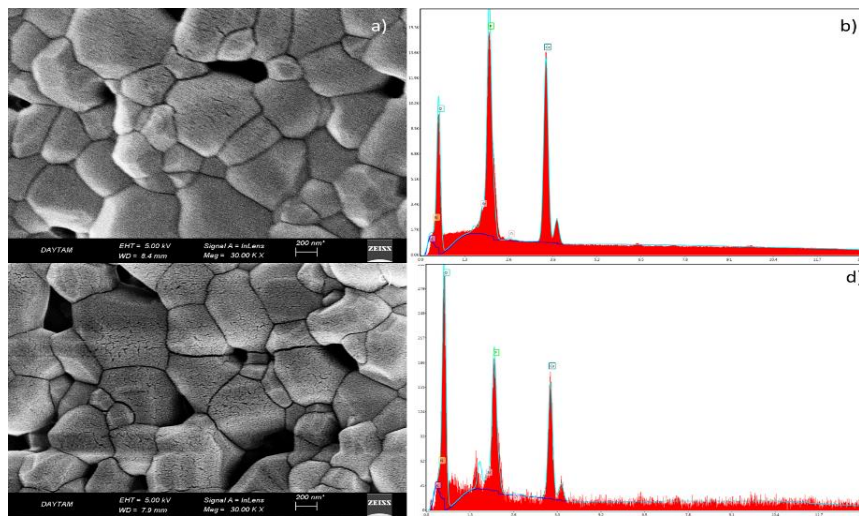


**Figure 7.** SEM and EDS images of synthesized samples (200nm). (a,b) 1.5TCP2.5Sr2.5Cl2.5F (c,d) 1.5TCP2.5Sr2.5Cl5.0F

Vickers micro-hardness measurements were obtained with Shimadzu HMV-G21 indentation tester (Table 3). Indentations were carried out using Vickers Micro-hardness indenter for load 1.916 N, over a time interval of 20 s. For each sample, several measurements were taken and average value of horizontal ( $L_1$ ) and vertical ( $L_2$ ) were used to calculate the micro-hardness. Average microhardness values found to be between 0.303 and 1.761 GPa which is similar to

the literature (Ramesh, 2000 and Suchamet et al. 1996) values (Cortical bone, 0.396 GPa, Cancellous bone, 0.345 GPa). Micro-hardness of the 1.5TCP 2.5Sr 1.0Cl 1.0F is much higher than human cortical bone. Co-doping of  $Sr^{2+}$ ,  $Cl^-$  and  $F^-$  resulted in reduced micro-hardness. Moreover, as the amount of  $Sr^{2+}$  ion in TCP structure was increased, micro-hardness values increased until sample 1.5TCP 5.0Sr 1.0Cl 1.0F.

**Table 2.** The densities of the TCP and doped TCP's sintered at 1100°C for 1 h.

Sample Names	Density (g cm <sup>-3</sup> )
1.5TCP	3.0433
1.5TCP 1.0Sr 1.0Cl 1.0F	2.9511
1.5TCP 2.5Sr 1.0Cl 1.0F	3.0450
1.5TCP 5.0Sr 1.0Cl 1.0F	2.8047
1.5TCP 10.0Sr 1.0Cl 1.0F	3.6444
1.5TCP 2.5Sr 2.5Cl 1.0F	2.5838
1.5TCP 2.5Sr 5.0Cl 1.0F	2.4979
1.5TCP 2.5Sr 10.0Cl 1.0F	2.7894
1.5TCP 2.5Sr 2.5Cl 1.0F	3.9766
1.5TCP 2.5Sr 2.5Cl 2.5F	4.0632
1.5TCP 2.5Sr 2.5Cl 5.0F	2.7955

**Table 3.** Mean of the Vickers hardness values of the samples.

Sample Names	Micro-hardness (GPa)
1.5TCP	1.208
1.5TCP 1.0Sr 1.0Cl 1.0F	1.502
1.5TCP 2.5Sr 1.0Cl 1.0F	1.761
1.5TCP 5.0Sr 1.0Cl 1.0F	1.306
1.5TCP 10.0Sr 1.0Cl 1.0F	0.416
1.5TCP 2.5Sr 2.5Cl 1.0F	1.408
1.5TCP 2.5Sr 5.0Cl 1.0F	0.554
1.5TCP 2.5Sr 10.0Cl 1.0F	0.713
1.5TCP 2.5Sr 2.5Cl 1.0F	0.303
1.5TCP 2.5Sr 2.5Cl 2.5F	1.418
1.5TCP 2.5Sr 2.5Cl 5.0F	1.623

## CONCLUSION

In the present study, we synthesize tri-calcium phosphates doped with strontium (Sr<sup>+2</sup>), chloride (Cl<sup>-</sup>) and fluoride (F<sup>-</sup>) ions for developing novel nanocomposite bioceramics. We have investigated the effects of strontium (Sr<sup>+2</sup>), chloride (Cl<sup>-</sup>) and fluoride (F<sup>-</sup>) doped ions on the morphology of the synthesized TCP products. Based on the obtained results in this study, we draw the following conditions.

- The XRD patterns demonstrated that for CaP ratio 1.50 at 1100°C, β-TCP phase was observed.
- From XRD results, small shifts in peak positions were observed, due to the

incorporation of ions Sr<sup>+2</sup>, Cl<sup>-</sup> and F<sup>-</sup> increased the crystallinity.

- In the Sr<sup>+2</sup>, Cl<sup>-</sup> and F<sup>-</sup> doped samples of 1.50 TCP, decomposition of β-TCP, α-TCP and formation of CaO, SrCl<sub>2</sub> and CaF<sub>2</sub> observed.
- SEM images verified the sintering temperature and amount of dopants had important effect on the grain sizes of the doped samples.

According to the results, the average grain sizes of the doped samples decreased. With doping ions, average grain sizes in CaP ratio 1.50 raised. TCP with molar ratio of 1.50 doped with 1.0 to 2.5% mole Sr<sup>+2</sup>, 1.0 to 2.5% mole Cl<sup>-</sup> and 1.0% mole F<sup>-</sup> sintered at 1100°C were found the most outstanding materials for future biomedical applications.

## ACKNOWLEDGMENT

The author wish to acknowledge the funding from Van Yuzuncu Yil University, Scientific Research Projects Unit (The Project Code: BAP-FYL-2016-5431).

## REFERENCES

- Bose S, Fielding G, Tarafder S, and Bandyopadhyay A, 2013. Understanding of dopant-induced osteogenesis and angiogenesis in calcium phosphate ceramics. *Trends Biotechnol*, 31: 594-605.
- Carrodegua RG, De Aza S, 2011.  $\alpha$ -Tricalcium phosphate: synthesis, properties and biomedical applications. *Acta Biomater*, 7: 3536–3546.
- Cheng K, Weng W, Wang H, Zhang S, 2005. In vitro behavior of osteoblast-like cells on fluoridated hydroxyapatite coatings. *Biomaterials*, 26: 6288-95.
- Gross K, Rodriguez-Lorenzo LM, 2004. Sintered hydroxyfluorapatites: II. Mechanical properties of solid solutions determined by microindentation. *Biomaterials*, 25: 1385-94.
- Grynopas MD, Hamilton E, Cheung R, Tsouderos Y, Deloffre P, Hott M, Marie PJ, 1996. Strontium increases vertebral bone volume in rats at low dose that does not induce detectable mineralization defect. *Bone*, 18: 253-9.
- Kannan S, Goetz-Neunhoeffler F, Neubauer J, Ferreira JMF, 2008. Ionic substitutions in biphasic hydroxyapatite and  $\beta$ -tricalcium phosphate mixtures: structural analysis by Rietveld refinement. *Journal of the American Ceramic Society*, 91: 1-12.
- Kannan S, Rocha JHG, Ferreira JMF, 2006. Synthesis of hydroxychlorapatites solid solutions. *Mater. Lett.* 60: 864-868.
- Kutbay I, Yilmaz B, Evis Z, Usta M, 2014. Effect of calcium fluoride on mechanical behavior and sinterability of nano-hydroxyapatite and titania composites. *Ceramics International*, 40: 14817-14826.
- LeGeros R, Z, 2002. Properties of osteoconductive biomaterials: calcium phosphates. *Clinical orthopedics and related research*, 395: 81-98.
- LeGeros RZ, 2008. Calcium phosphate-based osteoinductive materials. *Chemical reviews*, 108: 4742-4753.
- Metseger D, Rieger RM, and Foreman DW, 1999. Mechanical properties of sintered hydroxyapatite and tricalcium phosphate ceramic. *Journal of materials science. Materials in medicine*, 10: 9-17.
- Nakade O, Koyama H, Arai J, Aiji H, Takada J, Kaku T, 1999. Stimulation by low concentrations of fluoride of the proliferation and alkaline phosphatase activity of human dental pulp cells in vitro. *Arch. Oral Biol.*, 44: 89-92.
- Taktak R, Elghazel A, Bouaziz J, Charfi S, Keskes H, 2018. Tricalcium phosphate fluorapatite as bone tissue engineering: evaluation of bioactivity and biocompatibility. *Mater. Sci. Eng. C*, 86: 121–128.
- Park JB, Lakes RS, 1992. *Characterization of Materials I*. Biomaterials, Springer-Verlag New York, 29-62.
- Ramesh S, 2000. Grain Size- Properties Correlation in Polycrystalline Hydroxyapatite Bioceramic, *Malaysian Journal of Chemistry*, 3: 0035 – 0040.
- Suchanek W, Yashima M, Kakihana M, and Yoshimura M, 1996. Processing and Mechanical Properties of Hydroxyapatite Reinforced with Hydroxyapatite Whiskers, *Biomaterials* 17: 1715-1723.
- Verberckmoes SC, 2004. Effects of strontium on the physicochemical characteristics of hydroxyapatite. *Calcified Tissue Int.* 75: 405-15.
- Zhao J, Dong X, Bian M, 2014, Solution combustion method for synthesis of nanostructured hydroxyapatite, fluorapatite and chlorapatite. *Appl. Surf. Sci.* 1026-1033.